

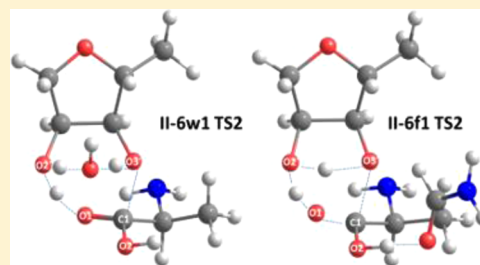
Theoretical Study on Two-Step Mechanisms of Peptide Release in the Ribosome

Carles Acosta-Silva, Joan Bertran,* Vicenç Branchadell, and Antoni Oliva

Departament de Química, Universitat Autònoma de Barcelona, 08193 Bellaterra, Spain

S Supporting Information

ABSTRACT: A quantum mechanical study of different two-step mechanisms of peptide release in the ribosome has been carried out using the M06-2X density functional. Reoptimization with MP2 has also been carried out for the stationary points of some selected mechanisms. The uncatalyzed processes in solution have been treated with the SMD solvation model. From the results obtained in this paper for the peptide release process we can conclude that the energy barriers for the two-step mechanisms are lower than the ones for the concerted process, that the 2'OH plays also an important role in the catalytic process and that the side chain does not only accommodate a nucleophilic water molecule in the PTC, but it also contributes to activate this molecule through electron transfer to the water oxygen. We have also found that the second step is the rate-determining one, and that the two most favorable mechanisms, in which a water or a formamide molecule is added, follow a quite different strategy to catalyze the reaction. The main conclusion of our work is that the two-step mechanisms cannot be disregarded, since they can contribute to clarify the complex and yet unsolved problem of the mechanism of the peptide release process.



■ INTRODUCTION

The active site of the ribosome, the peptidyl transferase center (PTC), catalyzes two reactions in the synthesis of proteins. On one side, peptide bonds are formed by the nucleophilic attack of an aminoacyl-tRNA in the A-site on peptidyl t-RNA in the P-site. The other reaction is the release factor dependent hydrolysis of peptidyl t-RNA.^{1,2} The release factors RF1 and RF2 are proteins that contain a GGQ tripeptide that interacts with the ribosomal PTC. It has been assumed that the GGQ motif triggers the hydrolysis reaction. However, in the isolated crystal structures, the release factors are in a compact form and the distance between the decoding center (DC) and the PTC seems too long to allow the role of the GGQ motif. This problem was solved when several studies^{3–11} showed that the ribosome-bound RF1 and RF2 adopt an “open” conformation. The role of RFs in codon recognition has encouraged the idea that these proteins may mimic tRNA molecules both in size and shape in such a way that they may produce identical conformational changes in the ribosome.^{2,4,6,9}

In a recent paper,¹² we carried out a quantum mechanical study of the concerted mechanism of the peptide release hydrolysis in the ribosome. Our purpose was to clarify whether the peptide release hydrolysis and the peptide bond formation take place through similar mechanisms and transition states. For this reason, we used the same methodology than in a previous study¹³ of the peptide bond formation process. One of our conclusions was that the 2'OH plays a much more important role in the proton shuttle mechanism in the peptide release process than in the peptide bond formation. This different behavior is in excellent agreement with the recent experimental results of the Strobel and Green's group,¹⁴ which show that the 2'OH plays a

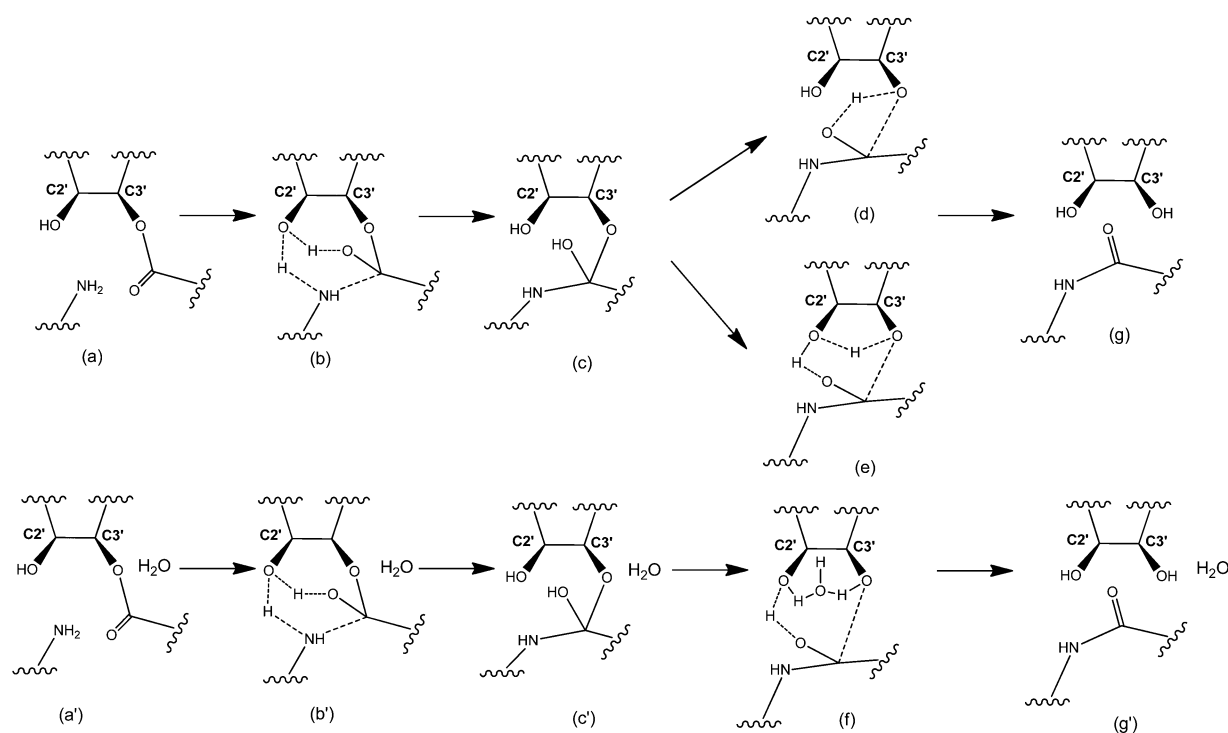
quite different role in the mechanism of both processes, thus correcting previous works^{15,16} in which some authors affirmed that the proton shuttle mechanism had a similar role in both processes. Another interesting result of our work is that the formation of an eight-membered ring cycle when one water molecule is hydrogen bonded to both O2' and O3' makes both processes more favorable. This mechanism was first proposed by the group of Steitz¹⁷ using high-resolution (2.3–2.7 Å) X-ray data for the active center of peptidyl transferase reaction. In the same paper, a second water molecule was found near the O1 atom in such a way that it can play the role of an oxyanion hole. For the peptide release process, the position of the water molecules has not been detected, since X-ray studies have been carried out with a resolution of only 3–3.5 Å.^{18–21} Nevertheless, molecular dynamics studies^{22–25} showed the presence of these two water molecules in both reactions.

It is also worth mentioning our results about the mechanism by which the GGQ motif triggers peptidyl-tRNA hydrolysis. Experimental studies lead to two different possibilities. On one side, some authors^{18,21,26} proposed that the glutamine residue of GGQ adopts a conformation in which the side chain accommodates a water molecule in the PTC. Other authors^{19,20,27} proposed that the main-chain NH of the glutamine is positioned to participate in the catalysis by forming a hydrogen bond with the oxyanion at the transition state. We showed that the lateral chain not only orientates the water molecule for the nucleophile attack but also activates this

Received: February 4, 2014

Revised: April 30, 2014

Published: May 6, 2014

Scheme 1. Schematic Representation of the Studied Two-Step Mechanisms for the Peptide Bond Formation^a

^a(a and a') reactants, (b and b') first transition states, (c and c') intermediates, (d, e, and f) second transition states, (g and g') products.

molecule. The role of the main-chain NH as an oxyanion hole was also confirmed in our work, but we found that this role could also be played by a water molecule. On the contrary, we previously found¹³ that water does not act as an oxyanion hole in TS of the peptide bond formation process, in good agreement with a recent experimental observation.²⁸

Another important point that deserves some discussion is the fact that the barriers obtained in our paper¹² for the concerted mechanisms of the peptide release process were clearly overestimated, thus leading to rate constants much lower than the experimental ones.^{3,29} We attributed this overestimation to the methodological limitations which are inherent in quantum-mechanical studies of complex systems, especially the use of a reduced model of the real system. This reduced model might not take into account the mechanical and electrostatic embedding due to the enzyme. However, the overestimation of the energy barriers could also be due to the fact that we only studied concerted mechanism, two-step mechanisms also being possible.

For the related peptide bond formation, following an idea of Rangelov et al.,³⁰ Wang et al.³¹ carried out a B3LYP study of a two-step mechanism (Scheme 1) in which the A76 2'-OH group transfers one proton to the carbonyl oxygen atom while, simultaneously, it receives one proton from the α -NH₂ group in such a way that a six-membered ring is formed (a). Protonation of the carbonyl oxygen neutralizes the negative charge of the oxyanion, thus leading to a neutral intermediate (b). In a second step, the proton is transferred to the O3' leaving group, and the system adopts a four-membered ring structure (c). We carried out¹³ a M06-2X study of the same mechanism and of two other ones, whose second steps lead to six-membered ring (d) and eight-membered ring (e) structures. In the last one, a water molecule was added throughout the process. Another M06-2X study on the mechanism leading to the six-membered ring (d) has recently been carried out by Byun and Kang³² using a larger

model than the one we used. Their model adds two water molecules and the A2451 fragment to the model we used, which does not seem to play a fundamental role in the mechanism, since their energy profiles are very similar to the ones obtained by Wang³¹ and in our paper.¹³

To our knowledge, no quantum-mechanical (QM) works have been devoted to the study of two-step mechanisms for the peptide release process. The purpose of this work is just to carry out such a study in order to compare it with the concerted mechanisms that we already discussed in our previous work.¹²

■ COMPUTATIONAL METHODS

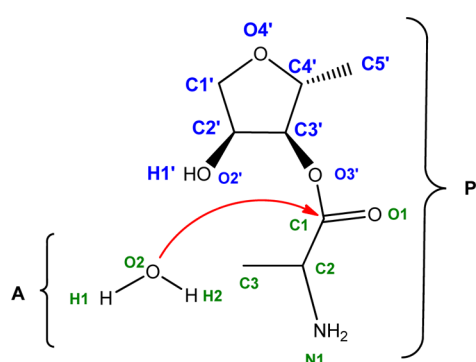
Given that we want to compare the results obtained for both mechanisms, the same methodology will be used throughout the present paper. So, the calculations have been carried out using the M06-2X functional proposed by Truhlar's group,^{33,34} a highly parametrized metahybrid method. Reoptimization with MP2 has also been carried out for the stationary points of some selected mechanisms. All the calculations have been done using the triple- ζ 6-311+G(d,p) basis set. The introduction of the solvent effect has been carried out using the SMD method of Marenich et al.³⁵ SMD is a universal solvation model, where "universal" denotes its applicability to any charged or uncharged solute in any solvent or liquid medium for which a few key descriptors are known. Thermochemical corrections to the energy values have been computed using the standard rigid rotor/harmonic oscillator formulas.³⁶ Relative Gibbs energies in solution have been computed with 1 mol L⁻¹ at a temperature of 298.15 K used as the reference state.

All quantum-mechanical calculations have been performed using Gaussian 09,³⁷ and the stationary points have been fully characterized. Full natural bond orbital analysis has been carried out with NBO version 3.³⁸

The reduced model we have adopted to represent the complex system is also the same as in our previous paper, and it is based in the philosophy of the theozymes (theoretical enzymes) proposed by Tantillo et al.³⁹ In this way, the group of Houk carried out^{40,41} theoretical studies of several enzymatic processes and they have obtained transition structures without any constraint, which are quite close to the X-ray transition state analogues. This structural agreement between the theozyme and the real enzyme is in accord with the paradigm wherein the enzyme structure assumes a maximum free energy lowering of the transition state. It is also worth mentioning that theozymes are also used in the computational design of artificial enzymes.^{42–44}

Scheme 2 depicts the basic model, which includes the atoms that intervene in all the mechanisms we have studied. The main

Scheme 2. Schematic Drawing Showing the Reactants in the Nucleophilic Attack of a Water Molecule at A-site on the Carbonyl Group of the Ester Formed between the Peptide Chain and tRNA at P-site^a



^aThis numbering of atoms will be used throughout the paper.

simplifications in our model can be summarized as follows. The atom C5', which in the real system is bonded to the oxygen atom of a phosphate in the RNA main chain has been represented by a methyl group. The base bonded to the C1' has been modeled by a hydrogen atom. The methyl group C3 represents the lateral chain of an amino acid. In the amino group, N1 one of the hydrogen atoms takes the place of a polypeptide chain. Only the

three hydrogen atoms which intervene in the process are explicitly shown and numerated.

As X-ray data show that the amide groups present in the lateral^{18,21} or in the main chain^{19,20,27} of glutamine in the GGQ motif play an important role in the enzymatic process and molecular dynamics (MD) studies^{24,25} indicate that additional water molecules can also be relevant, additional water or formamide molecules have been explicitly considered in some cases.

For the peptide release process, there is a lack of experimental and theoretical information about transition state geometries. For this reason, we have located the transition states starting from the equivalent structures in the peptide bond formation process (Scheme 1) with the obvious exception of the nucleophile (a water molecule instead of the amino group). For each transition state, the intrinsic reaction coordinate⁴⁵ (IRC) was calculated. The final points of each reaction path were used to fully characterize the reactant and product complexes associated with each transition state through a complete optimization. Finally, the isolated reactants and products were also optimized. It is worth mentioning that no geometry constraints have been used in any step of our study.

RESULTS

We have considered different two-step mechanisms. In the first step of all of them, the nucleophilic attack is accompanied by a proton transfer from O2 to O1, while in the second step, a proton is transferred from O1 to O3', simultaneously with the cleavage of the C1–O3' bond (see Scheme 3). If both transfers proceed in a direct way, the two transition states have a 4-membered ring (mechanism II-4), but if they take place through the hydroxyl group linked to C2', the geometries of the transition states contain a six-membered ring cycle (mechanism II-6). As mentioned above, the amide groups present in the lateral or in the main chain of glutamine in the GGQ motif play an important role in the enzymatic process and, thus, additional water molecules can also be relevant. For this reason, we have also studied four additional mechanisms by introducing a water or a formamide molecule which interacts with the hydrogen atom of the nucleophilic water molecule (mechanisms II-6w1 and II-6f1) or which acts as an oxyanion hole of the O1 carbonylic atom (mechanisms II-6w2 and II-6f2). It is worth mentioning that the

Scheme 3. Schematic Representation of the Studied Two-Step Mechanisms II-4 and II-6 Corresponding to the Peptide Release Process

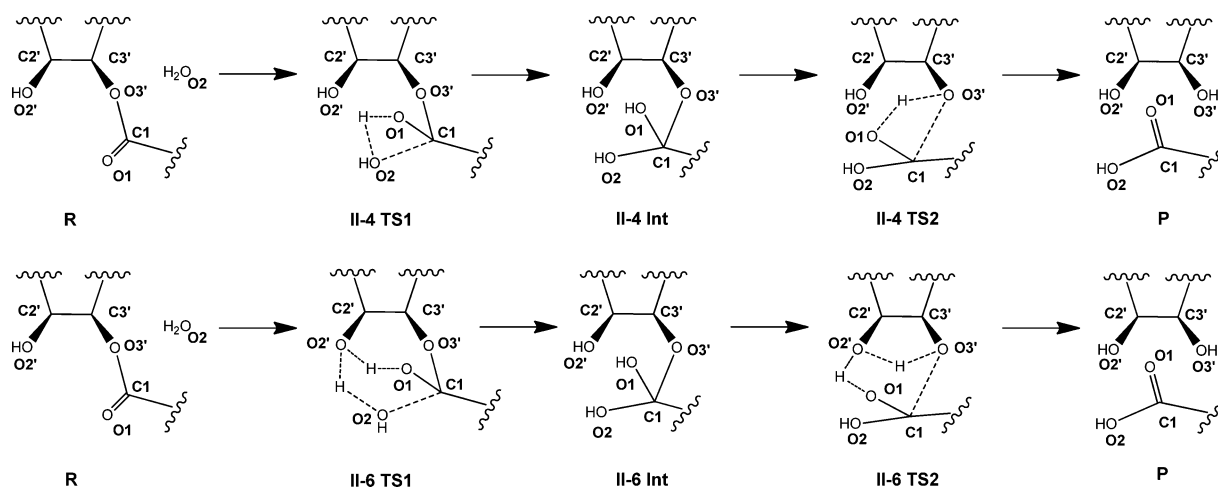


Table 1. Summary of Relative Energies (kcal mol⁻¹) at the M062X/6-311+G(d,p) Level of Calculation for the Two-Step Mechanisms. Values in Parentheses Correspond to the MP2/6-311+G(d,p) Level of Calculation

mechanism	energy	R	RC	TS1	Int1	Int2	TS2	PC	P
II-4	ΔE	0.0	-5.4 (-8.1)	37.5 (40.4)	-1.7 (3.1)	-0.6 (5.9)	39.8 (44.6)	-4.3 (-1.0)	6.0 (8.2)
	ΔH	0.0	-3.8 (-6.5)	35.8 (38.9)	0.4 (5.2)	1.8 (8.3)	38.2 (43.2)	-2.2 (1.0)	6.6 (8.8)
	ΔG	0.0	4.6 (1.9)	47.8 (50.8)	12.2 (16.6)	14.4 (20.4)	50.0 (55.2)	7.4 (10.0)	4.7 (6.7)
II-6	ΔE	0.0	-9.1 (-8.9)	25.8 (28.9)	-4.8 (0.1)	-4.8 (0.1)	29.9 (31.4)	-6.9 (-4.2)	7.2 (9.1)
	ΔH	0.0	-7.4 (-7.1)	23.0 (26.2)	-2.4 (2.5)	-2.4 (2.5)	27.7 (29.1)	-4.6 (-2.1)	7.8 (9.7)
	ΔG	0.0	2.5 (1.8)	37.0 (40.8)	10.2 (15.2)	10.2 (15.2)	40.9 (43.4)	5.5 (7.9)	5.7 (8.1)
II-6S	$\Delta E'$	0.0	-6.1	29.3	2.5	2.0	36.2	-2.5	2.8
	$\Delta H'$	0.0	-4.5	26.8	5.1	4.6	34.3	-0.5	3.9
	ΔG	0.0	3.7	39.8	15.8	15.0	46.7	6.9	2.6
II-6w1	ΔE	0.0	-13.6 (-12.1)	16.5 (20.9)	-11.9 (-5.1)	-11.7 (-5.1)	21.7 (27.7)	-10.8 (-7.2)	2.9 (6.8)
	ΔH	0.0	-11.6 (-9.9)	14.4 (18.8)	-9.1 (-2.5)	-9.2 (-2.4)	18.3 (24.1)	-8.5 (-4.8)	3.8 (7.7)
	ΔG	0.0	-0.5 (1.2)	30.5 (35.3)	5.2 (11.7)	4.3 (11.6)	33.7 (39.7)	1.5 (5.9)	2.5 (6.7)
II-6w2	ΔE	0.0	-9.8	24.2	-5.1	-5.1	28.0	-7.3	2.9
	ΔH	0.0	-8.2	21.5	-2.9	-2.9	25.8	-5.4	3.7
	ΔG	0.0	2.4	35.9	9.7	10.0	40.0	5.3	3.0
II-6f1	ΔE	0.0	-14.4 (-9.1)	15.2 (22.2)	-11.8 (-3.5)	-11.8 (-3.5)	23.5 (29.2)	-13.7 (-7.2)	2.0 (7.8)
	ΔH	0.0	-12.4 (-7.1)	12.9 (20.0)	-9.4 (-1.1)	-9.4 (-1.1)	20.6 (26.5)	-11.7 (-5.0)	2.5 (8.5)
	ΔG	0.0	-0.6 (2.9)	28.6 (35.0)	4.4 (11.7)	4.4 (11.7)	34.4 (39.3)	-1.2 (3.9)	0.0 (5.4)

second TS structure of mechanism II-6w1 presents an eight-membered cycle, while the one corresponding to mechanism II-6f1 keeps the six-membered cycle. On the other side, the direct location of the first-step transition structure of mechanism II-6f2 leads to a structure which is very similar to the transition state of mechanism II-6f1 in such a way that the II-6f2 one has been disregarded. Finally, we have tried to introduce the solvent effect on mechanisms II-4 and II-6 by using the SMD method. For mechanism II-4, the solvent effect leads to an ion pair through a heterolytic breaking of the C1–O3' bond, but the transition vector of TS2 indicates that there is no proton transfer. So, we will only study the solvent effect on mechanism II-6 (referred as II-6S from now on). For each one of the above-mentioned mechanisms, the energy values, the geometry parameters of the stationary points, and the charge distribution will be successively analyzed.

Table 1 shows the variation, with respect to the isolated reactants (R), of the potential energy, the enthalpy, and the Gibbs free-energy corresponding to the reactant complex (RC), the transition states (TS1 and TS2), the intermediates between both transition states (Int1 and Int2), the product complex (PC),

and the isolated products (P) for the six studied mechanisms. The choice of the separated reactants (R) as the reference for the energies reported in Table 1 is consistent with the fact that we are studying the bimolecular process in order to compare the obtained values to the ones of our previous studies for the aminolysis which intervenes in the peptide bond formation process.

The optimizations have been carried out using the M06-2X functional. The stationary points of the four most relevant mechanisms have also been optimized at the MP2 level. One can observe that the relative energies obtained with MP2 are slightly higher than the M06-2X ones and that they keep the same ordering at both levels, thus confirming that the choice of this functional was adequate. In all cases, the second transition structure (TS2) lies higher in energy than the first one (TS1), in such a way that it is the rate-determining step for the whole process. If one looks at the energy values corresponding to the isolated products (P), one can observe that all reactions are slightly endothermic. Furthermore, the enthalpy and the Gibbs free energy are very similar, thus implying a small value of the entropy term as it was to be expected given the presence of two

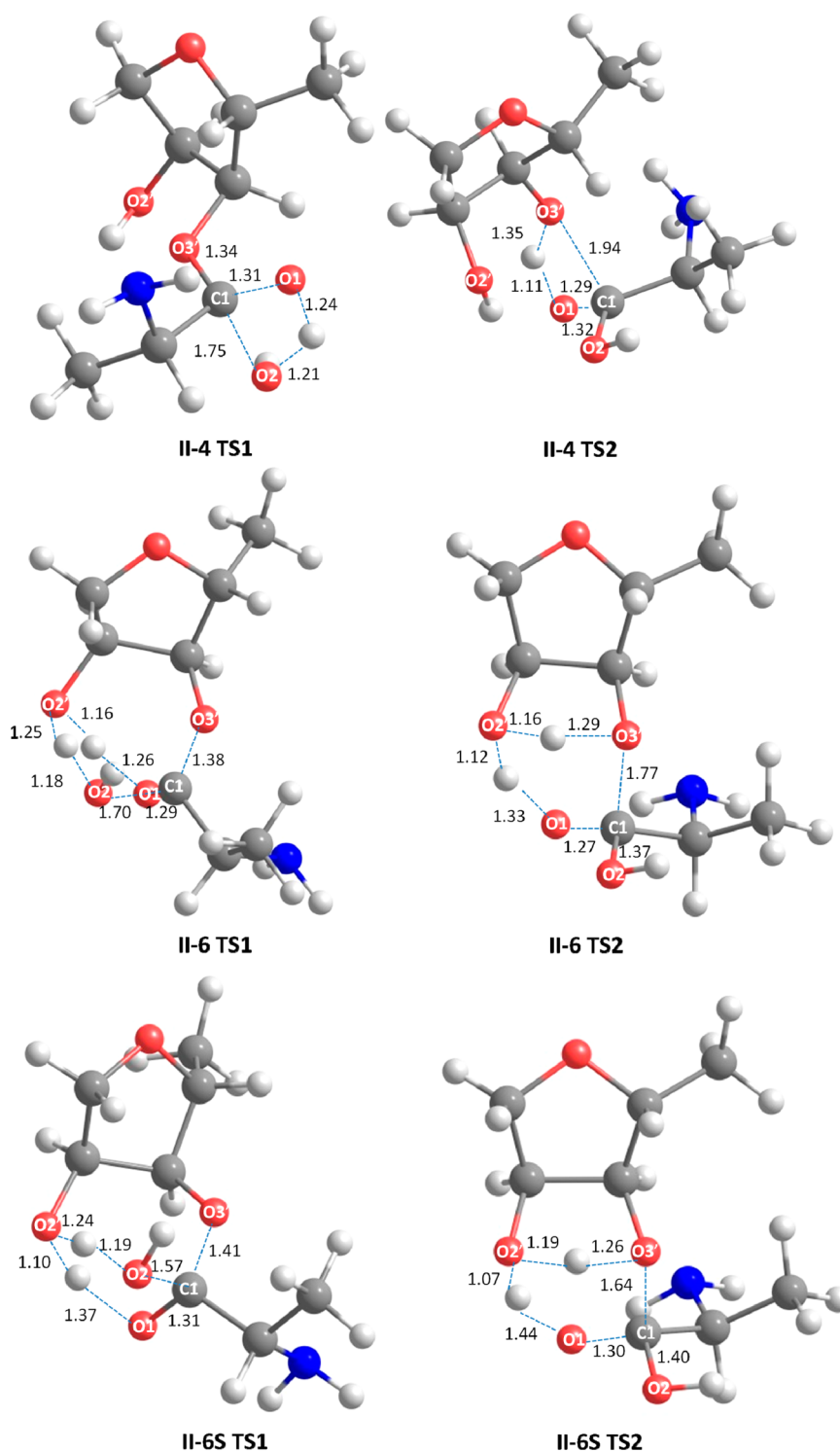


Figure 1. Transition state structures for the two-step mechanisms II-4, II-6, and II-6S. Selected interatomic distances are in Å.

molecules in the isolated reactants and products. On the contrary, the entropy term is clearly positive in the complexes, transition structures, and intermediates, since there is now one molecule instead of the two in the isolated reactants. In fact, the positive value of the entropy term comes from the conversion of six translational and rotational degrees of freedom into vibrations and pseudorotations. As a direct consequence, the free-energy values of the reactant complexes (RC) are usually positive, a fact which is surprising since RC plays the role of the Michaelis complex, which, as it is well-known, is thermodynamically stable.

This can be attributed to the simplified model we are using, which does not take well into account the ability of the real system to act as an entropic trap.⁴⁶ The presence of two intermediates (Int1 and Int2) in Table 1 is due to the methodology we have used to obtain them. As indicated in the method of calculation, the intermediates Int1 and Int2 have been identified through the calculation of the IRC starting from TS1 and TS2, respectively. In fact, the two intermediates correspond to different conformers of the same chemical species. In all cases, the energy values of both intermediates are very similar, thus

suggesting that the energy barrier between them should be negligible.

With regard to the energy barriers of the different mechanisms, Table 1 shows that both steps of mechanism **II-6** are more favorable than the corresponding ones in mechanism **II-4**, the difference in energy barriers being around 10 kcal mol⁻¹. This implies that the substrate assisted catalysis favors the formation of a six-membered ring cycle. In mechanism **II-6S**, where the solvent effect has been introduced, the energy and enthalpy are indicated as E' and H', since the computed energy is obtained by adding free energy of solvation to gas-phase potential energy surface. In contrast, G is the real free energy as it contains the free energy of solvation. It has to be emphasized that complete optimization has been done for all the stationary points in the E' energy surface, instead of merely adding the solvation energy to the optimized gas-phase structures.⁴⁷ The energy barrier corresponding to the second step is about 7 kcal mol⁻¹ higher than the one for the **II-6** mechanism, in quite good agreement with the value of 6–7 kcal mol⁻¹, which can be calculated from the experimental rate constants.^{3,29} The different energy values of the intermediates are related to the conformations of these structures and will be discussed below.

Let us now consider the two mechanisms in which a water or a formamide molecule interact with the hydrogen atom of the nucleophilic water molecule (mechanisms **II-6w1** and **II-6f1**). One can observe in Table 1 that the energy barrier of the first step (TS1) notably decreases from 25.8 to 16.5 kcal mol⁻¹ in the case of water and to 15.2 kcal mol⁻¹ in the case of formamide. The same trend can be observed for the rate-determining second step since the energy of TS2 decreases from 29.9 to 21.7 and 23.5 kcal mol⁻¹, respectively. It is also worth mentioning that the second-step activation enthalpies of mechanisms **II-6w1** and **II-6f1** (18.3 and 20.6 kcal mol⁻¹, respectively) are in quite good agreement with the ones corresponding to the experimental values of the rate constants.^{3,29} Finally, the results obtained for mechanism **II-6w2**, in which the water molecule acts as an oxyanion hole of the O1 carbonylic atom, show that the effect on the energies of both transition states is quite small, a fact that could be expected since O1 is involved in the proton transfer process in both steps.

The geometries of the transition structures of all the studied mechanisms are shown in Figures 1 (mechanisms **II-4**, **II-6**, and **II-6S**) and 2 (mechanisms **II-6w1**, **II-6w2**, and **II-6f1**). For the two transition structures and the two intermediates of the six mechanisms, Table 2 presents the C3'O3'C1O2 dihedral angle (whose sign shows the side in which the attack is produced), the Wiberg bond index⁴⁸ for the C1–O1 bond, and the value of T(C1), which is a measure of the tetrahedral character of the geometry around C1 and whose value is obtained as the sum of the six bond angles around this carbon atom. T(C1) is expected to be 657° in a sp³ hybridization scheme and 630° when the sp² hybridization of the C1 atom is maintained while the attacking or leaving groups are far away.

Figures 1 and 2 show that all the transition states present 6-membered ring cycles except in three cases: both transition states of mechanism **II-4** (where the cycle is a four-membered ring) and the TS2 of mechanism **II-6w1** (whose structure presents an eight-membered ring cycle). The intermediates correspond to diol species, since the C1–O1 bonds already have a single bond character as can be observed in Table 2 from the values of the Wiberg Indexes (which vary from 0.93 to 0.98) and from the tetrahedral character around the C1 atom, the T(C1) values being very close to 657° in all cases. In fact, the C1–O2 bonds are already formed in the intermediates, their bond lengths being

Table 2. C3'O3'C1O2 Dihedral Angle, Wiberg Index of the C1–O1 Bond and Tetrahedral Character of the Structure Around the C1 Atom, T(C1), for the Transition States and Intermediates of the Six Studied Mechanisms

mechanism	structure	dihedral angle (C3'O3'C1O2)	Wiberg index (C1–O1)	T(C1)
II-4	TS1	–88.6	1.18	651.7
	Int1	–71.4	0.93	656.7
	Int2	–49.7	0.98	656.9
	TS2	21.7	1.19	648.2
II-6	TS1	–99.3	1.26	653.8
	Int1	–146.5	0.98	656.8
	Int2	–146.5	0.98	656.8
	TS2	–164.4	1.31	653.8
II-6S	TS1	–94.9	1.18	655.4
	Int1	–109.6	0.96	658.8
	Int2	–145.8	0.96	656.7
	TS2	–171.0	1.24	655.1
II-6w1	TS1	–95.8	1.21	655.0
	Int1	–149.3	0.96	656.9
	Int2	–153.2	0.96	656.8
	TS2	–150.1	1.38	652.2
II-6w2	TS1	–100.0	1.21	654.2
	Int1	–147.5	0.95	656.8
	Int2	–147.5	0.95	656.8
	TS2	–161.9	1.24	654.5
II-6f1	TS1	–98.8	1.20	655.4
	Int1	–113.6	0.97	656.9
	Int2	–113.6	0.97	656.9
	TS2	–156.1	1.30	648.3

very similar to those of the C1–O1 bonds. Table 2 also shows that TS1 and TS2 have an important tetrahedral character around the C1 atom, the value of T(C1) being slightly higher in the first transition state. With regard to the C3'O3'C1O2 dihedral angles, one can observe that they are always negative except the one corresponding to the TS2 of mechanism **II-4**. So, except in this latter case, the attack proceeds via a S chirality.

Let us consider the geometries depicted in Figure 1. For mechanism **II-4**, one can observe that in TS1 there is a proton transfer from O2 to O1, while in TS2 the proton is transferred from O1 to O3', the transfer being more advanced in the first transition state. As a direct consequence, the C1–O1 bond is losing and recovering its double bond character in TS1 and TS2, respectively. One important point that deserves to be mentioned is the evolution of the C1–O2 bond, which is the one that is formed in the nucleophilic attack. One can observe that this bond is not yet formed in TS1 (since the C1–O2 bond length is still 1.75 Å), while the bond length has decreased to 1.32 Å in TS2, thus presenting some double bond character. As a direct consequence, the C1–O3' bond is completely broken in TS2, its bond length value being 1.94 Å. For mechanism **II-6**, the proton transfers from O2 to O1 and from O1 to O3' take place through the hydroxyl group linked to C2'. Figure 1 shows that in TS1 the degree of transfer from O2 to O2' and from O2' to O1 are quite similar, while the transfer from O1 to O2' is more advanced than the one from O2' to O3' in TS2. In solution (mechanism **II-6S**), the solvent favors the nucleophilic attack in TS1 in such a way that the second transfer, from O2' to O1, is delayed with respect to the other one, while the transfer from O1 to O2' is clearly advanced in TS2. It is also worth mentioning that the solvent

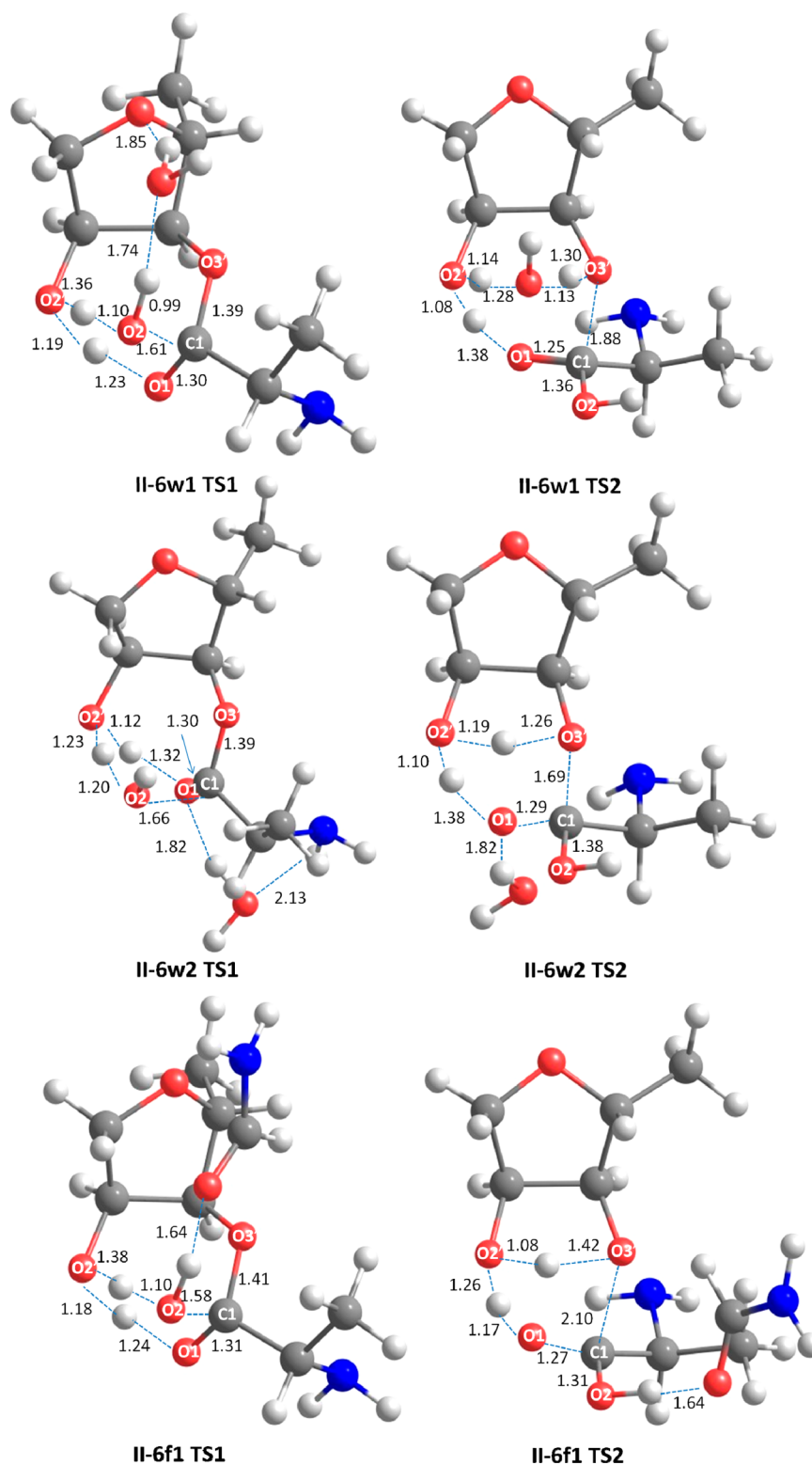


Figure 2. Transition state structures for the two-step mechanisms II-6w1, II-6w2, and II-6f1. Selected interatomic distances are in angstroms.

effect produces a lengthening of the bonds C1–O1 and C1–O2, the breaking of the C1–O3' bond being thus reduced.

With regard to the different energy values observed in Table I, Int1 in mechanisms II-4 and II-6 (and also those for Int2) are directly related to the corresponding geometry conformations. Figure 3 presents these four geometries, in which some selected atomic distances are shown. One can observe that the

conformations of Int1 and Int2 are quite different for both mechanisms. The same occurs when the two intermediates of mechanism II-4 are considered (it is worth remembering that both intermediates are found through the IRC from TS1 and TS2, respectively). On the contrary, the conformations of Int1 and Int2 are exactly the same for mechanism II-6, thus explaining that they have the same energy (see Table 1).

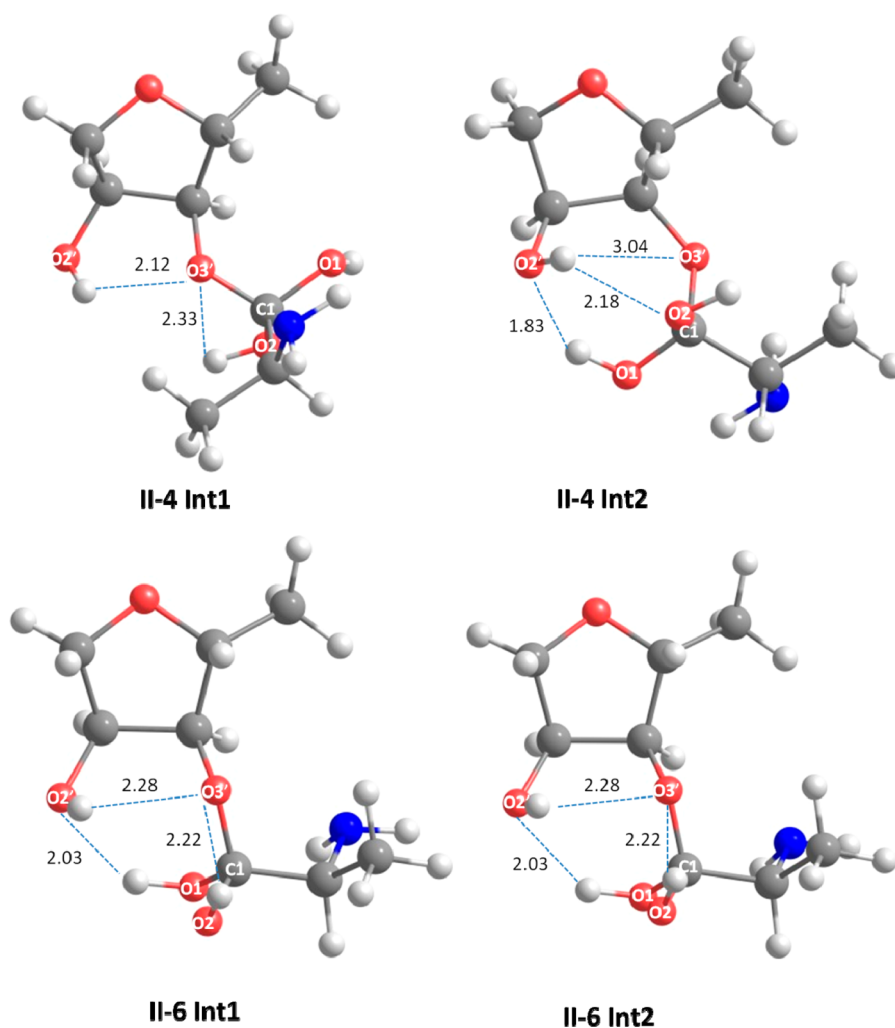


Figure 3. Intermediate structures for mechanisms II-4 and II-6. Selected interatomic distances are in angstroms.

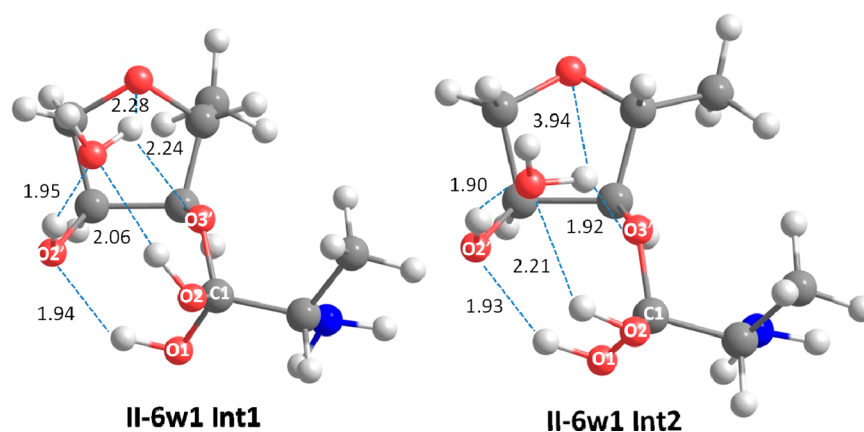


Figure 4. Intermediate structures for the mechanism II-6w1. Selected interatomic distances are in Å.

The transition structures of the other three studied mechanisms are presented in Figure 2. The TS1 of mechanisms II-6w1 and II-6f1 are quite similar, the oxygen atom of the water or formamide molecules being hydrogen bonded to the nucleophilic water through the hydrogen atom which is not implied in the proton transfer. These hydrogen bonds increase the nucleophilic character of water as one can observe from the natural charges on the O2 atom of the reactant complex of

mechanisms II-6, II-6w1, and II-6f1 mechanisms (−0.969, −0.983, and −0.979, respectively) and from the bond lengths of the O2–C1 bond in the first transition state (TS1), whose values are 1.61 and 1.58 Å with water and formamide, respectively, much lower than the value of 1.70 Å in mechanism II-6. As a direct consequence, the proton transfer to O2' is delayed. However, this similarity between both mechanisms is not complete, since the water molecule is hydrogen bonded to the

oxygen atom of the sugar, while the amino group of formamide is about 3.12 Å away from this oxygen atom. With regard to the second step, the TS2 of both mechanisms are very different. In mechanism **II-6f1**, the six-membered ring cycle is maintained and the formamide molecule is still interacting with the hydrogen atom of the nucleophilic water molecule. On the other side, an eight-membered ring cycle is formed in mechanism **II-6w1**, since the hydrogen bonds with O2 and the sugar oxygen atom are now directed to O2' and O3', respectively. This change in the network of hydrogen bonds can easily be observed in intermediates Int1 and Int2 (see Figure 4). Thus, in Int1, the water molecule is already more hydrogen bonded to O2' (1.95 Å) than to O2 (2.06 Å) and to O3' (2.24 Å) than to the sugar oxygen atom (2.28 Å). This evolution to the formation of the eight-membered ring of TS2 is much more advanced in Int2. Figure 2 shows that the C1O3' bond is already broken in the TS2 of mechanisms **II-6w1** and **II-6f1**, while Table 2 indicates that the double bond character of the C1O1 bond increases (see the Wiberg indexes) and the tetrahedral character around the C1 atom diminishes [the value of T(C1) has noticeably decreased]. One last remark about the catalytic effect in mechanism **II-6f1**: the strong hydrogen bond between O2 and the formamide molecule contributes to the increase of the double bond character of the C1O2 bond (the bond lengths being 1.31 and 1.36 Å in mechanisms **II-6f1** and **II-6w1**, respectively) and to the breaking of the C1O3' bond (its length increasing from 1.88 to 2.10 Å when water is replaced by formamide). Finally, the presence of the water molecule in mechanism **II-6w2** has a small catalytic effect, since, as one can observe in Figures 1 and 2, both transition states are very similar to the ones of the **II-6** mechanism; the only aspect that can be mentioned is that the proton transfer to O1 is delayed in TS1, while in TS2 the proton transfer from O1 is advanced.

Table 3 presents the dipole moments, μ , and the natural atomic populations, q , on the O2, O3', O1, and O2' atoms for the

Table 3. Dipole Moment (μ , in D) and Relevant Natural Charges (q , in a.u.) for the Transition States of the Studied Mechanisms

TS	μ	$q(\text{O2})$	$q(\text{O3}')$	$q(\text{O1})$	$q(\text{O2}')$
II-4 TS1	2.08	−0.88	−0.63	−0.84	−0.73
II-4 TS2	1.89	−0.68	−0.86	−0.77	−0.76
II-6 TS1	1.66	−0.82	−0.64	−0.80	−0.78
II-6 TS2	2.73	−0.73	−0.75	−0.80	−0.74
II-6S TS1	2.74	−0.79	−0.67	−0.90	−0.78
II-6S TS2	4.28	−0.79	−0.70	−0.90	−0.75
II-6w1 TS1	3.43	−0.80	−0.65	−0.82	−0.82
II-6w1 TS2	2.27	−0.72	−0.80	−0.78	−0.74
II-6w2 TS1	2.38	−0.81	−0.65	−0.86	−0.77
II-6w2 TS2	1.55	−0.74	−0.71	−0.86	−0.74
II-6f1 TS1	5.42	−0.79	−0.67	−0.82	−0.82
II-6f1 TS2	4.68	−0.72	−0.88	−0.74	−0.76

transition structures of the six studied mechanisms. The dipole moments do not notably differ among the different transition states; the greatest values corresponding to mechanism **II-6f1**, in which a formamide molecule has been included. As was expected, the introduction of the solvent effect (mechanism **II-6S**) appreciably increases the dipole moments of the two transition states. The natural charges on O2 in the first transition state are correlated with the degree of advance of the nucleophilic attack (the more negative the charge, the longer the O2–C1 bond

length and so the less advanced the nucleophilic attack). Similarly, the natural charges on O3' in the second transition state is correlated with the heterolytic breaking of the C1–O3' bond (the more negative the charge, the longer the C1–O3' bond length). With regard to the natural charges over O1, one can observe that they are more negative than that over O3' in the first transition state. This fact implies that the charge transfer from O2 goes mostly to O1, which thus explains why the C1–O1 bond is losing its double bond character. In the second transition state, the natural charge over O3' is greater than over O1 in the three mechanisms (**II-4**, **II-6w1**, and **II-6f1**) in which the C1–O3' bond is more broken (see Figures 1 and 2), while the contrary occurs in the other three mechanisms. This different behavior can be related to the fact that in the first three mechanisms, the natural charge on O1 is notably greater in TS1 than in TS2, while in the other three cases the charge is nearly the same in both transition states. One special case that deserves some attention is the second step of mechanism **II-6f1**, since, as can be observed, the charges on O1 and O2 are nearly the same, this fact being directly related to the similarity of the distances C1–O1 and C1–O2. Let us finally consider the natural charges over O2'. Except in mechanism **II-4**, in which O2' does not intervene in the proton shuttle process, the charge is greater in TS1 than in TS2, the difference being especially important in mechanisms **II-6w1** and **II-6f1**, in which the proton transfer from O2 to O2' is delayed.

DISCUSSION

As mentioned at the end of Introduction, the main goal of this work is to compare the two-step mechanisms in the peptide release reaction with the previously studied concerted ones.¹² A first point that deserves some discussion is the fact that the barriers obtained in the concerted mechanism were clearly overestimated, thus leading to rate constants much lower than the experimental ones.^{3,29} The potential energies of TS2, which are the highest transition state in the six studied two-step mechanisms (see Table I), are about 5 to 10 kcal mol^{−1} lower than the potential energy barriers of the corresponding concerted mechanisms. For instance, the potential energy barrier for the most favorable two-step mechanism, **II-6w1**, is 21.7 kcal mol^{−1}, while it is 32.1 kcal mol^{−1} in the equivalent concerted mechanism. It is worth mentioning that in both cases an eight-membered ring cycle is formed. If we consider mechanism **II-6f1**, in which a formamide molecule is introduced instead of a water molecule, the potential energy barrier decreases from 30.3 kcal mol^{−1} in the concerted mechanism to 23.5 kcal mol^{−1} in the two-step process (a six-membered ring cycle is now formed). The activation enthalpies of these two-step mechanisms (18.3 and 20.6 kcal mol^{−1}, respectively) are in a quite good agreement with the experimental values.^{3,29} In contrast, the activation free energies (33.7 and 34.4 kcal mol^{−1}, respectively) are still too high as it was to be expected since, in our reduced model, the restrictions on the translation and rotation degrees of freedom in the ribosome are not taken into account (this is the so-called entropic trap).

A second point to be considered is the role played by the 2'OH in the proton shuttle process. Our previous studies^{12,13} in the concerted mechanisms were in good agreement with the experimental results of Strobel and Green's group,¹⁴ since they showed that the 2'OH plays an important role in the proton shuttle in the peptide release process, while this role was not found in the peptide bond formation. The results obtained in the present work clearly confirm that the 2'OH also plays a very

important role in each one of the two steps of the peptide release process. Thus, the fact that the potential energy barriers for TS1 and TS2 are around 10 kcal mol⁻¹ lower in mechanism II-6 than in the II-4 provides an indicator that the intervention of the 2'OH favors both steps through its intervention in the proton shuttle process.

On the contrary, our results for the two-step mechanisms do not agree with the idea of the groups of Noller^{19,20,27} and Aqvist,²⁵ according to whom the catalytic effect is due to the formation of a hydrogen bond between the main-chain NH of the glutamine or a water molecule with the O1 atom of the oxyanion. As was mentioned above, mechanism II-6f2 had to be disregarded since it lead to the II-6f1 one, while the energy barriers of mechanism II-6w2 do not differ appreciably from the II-6 ones; this is due to the fact that the O1 atom is involved in the proton transfer which occurs in both steps.

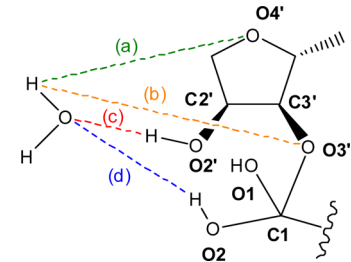
Finally, the fact that in the most favorable mechanisms we have found (II-6w1 and II-6f1), the oxygen atom of the water or formamide molecules is hydrogen bonded to the nucleophilic water through the hydrogen atom, which is not implied in the proton transfer and seems to confirm the ideas of the groups of Ramakrishnan^{18,21} and Aqvist,²⁵ which propose that the side chain accommodates a nucleophilic water molecule in the PTC. In fact, the formation of the hydrogen bond does not only accommodate the water molecule but also contributes to activate this molecule through electron transfer to the water oxygen. The presence of a water molecule interacting simultaneously with O2' and O3' in a RAP TS analogue of the peptide bond formation process was first found by Schmeing et al.¹⁷ from high-resolution X-ray experiments, and it was later confirmed through molecular dynamics studies.^{22,23} As mentioned in Introduction, the position of the water molecules was not detected for the reactants²¹ and products^{18–20} of the peptide release process because of the lack of resolution of the X-ray studies. However, the presence of this water molecule has been shown through molecular dynamics studies.^{24,25} Figure 2 shows that in the TS1 of mechanisms II-6w1 and II-6f1, the water or formamide molecules form a strong hydrogen bond with the nucleophile and another hydrogen bond with the O4' atom of the A76 sugar, this second interaction being quite weak in the case of formamide.

At this point, it is worth discussing the influence in this weak hydrogen bond of the reduced model we have used. The comparison with X-ray data shows that the NH₂ group of formamide is rather away from the O4' atom of the sugar, thus indicating that the interaction we have found is an artifact due to the simplicity of our model. In fact, X-ray data^{18,21} show that the amino group of formamide can form a hydrogen bond with the O2 atom of uracyl in the U2506 nucleotide, which is in the innermost layer of the active site of ribosome. The intervention of this nucleotide seems to be confirmed by a study⁴⁹ in which the mutation of uracyl reduces the catalytic effect on the peptide release process. However, given that the catalytic effect can be mainly attributed to the activation of the water molecule by the carbonyl group of formamide, the role played by the weaker interaction of the amino group with the O4' atom of the sugar or with the O2 atom of uracyl does not seem to be able to produce significant energy changes in the results of our work.

Let us now discuss the second step of the most favorable mechanisms (II-6w1 and II-6f1), which, as mentioned above, correspond to the rate-determining step. In both TS2 structures, the C1–O1 and C1–O2 bonds have some double bond character (stronger in C1–O1 than in C1–O2). This fact contributes to the breaking of the C1–O3' bond, which is greater

in mechanism II-6f1, given that formamide forms a hydrogen bond with the O2 atom. On the contrary, in mechanism II-6w1, the added water molecule has migrated and the equivalent hydrogen bond cannot be formed. So, both mechanisms follow a quite different strategy to catalyze the reaction. It is especially important to underline that the migration of the water molecule, which belongs to the protein structure, leads to the formation of an eight-membered ring cycle as can be clearly observed in Figure 4. To clarify this point, Table 4 presents the evolution of four

Table 4. Variation of Some Selected Distances between TS1 and Int1 for Mechanism II-6w1

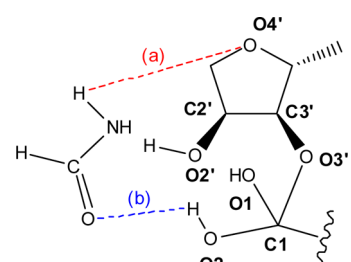


II-6w1	(a)	(b)	(c)	(d)
TS1	1.85	2.67	3.05	1.85
Int1	2.28	2.24	1.95	2.28
Δ	0.43	-0.43	-1.10	0.32

relevant distances from the TS1 to the Int1 for mechanism II-6w1. One can observe that while the distances from the oxygen of water to the hydrogen linked to O2 and from the hydrogen of water to the O4' atom of the sugar increase (depicted in blue and green, respectively), the distances from the oxygen of water to the hydrogen linked to O2' and from the hydrogen of water to the O3' atom decrease (depicted in red and yellow, respectively). This intrastep reorganization of the system leads to the interstep preorganization for the second step.⁵⁰ This preorganization is completed in the nearly isoenergetic equilibrium conformation between Int1 and Int2 (see Figure 4). The reorganization of the active center to prepare the formation of the eight-membered cycle reflects the coupling between the chemical process and the enzyme dynamics, a topic that is now at the heart of the debate.⁵¹

It is also worth mentioning that the reorganization implies a high mobility of the water molecule, this fact being possibly due to the reduced model we have used. The comparison between the two transition states of mechanism II-6f1 shows that this mobility is dramatically increased in the case of formamide (see Figure 2), this mobility being specially produced when Int2 transforms into TS2, as shown in Table 5, where the evolution of two relevant distances is presented. One can observe that the distance between the O atom of formamide and the H atom linked to O2 decreases (depicted in blue), while the hydrogen bond between one H atom of the amino group of formamide and the O4' atom of the sugar breaks completely (depicted in red). In this case, this can be attributed to the fact that, as mentioned above, our reduced model avoids the correct orientation of formamide, but it does not seem to be able to produce significant energy changes in the results of our work.

It has to be emphasized that the effect of the environment in the chemical processes is not well-introduced in the catalyzed reactions. As mentioned above, this implies that the system is allowed to be more flexible than it really is, since the constraints due to the physical environment are not taken into account. Moreover, the electrostatic embedding, due to the electrical field

Table 5. Variation of Some Selected Distances between Int2 and TS2 for Mechanism II-6f1


	(a)	(b)
Int2	2.65	1.85
TS2	6.14	1.64
Δ	3.49	-0.21

created by the enzyme, is poorly considered. A simplified way of introducing the electrical embedding is to mimic the environment through a medium with a value of the dielectric constant equal to 4,⁵² although some authors argue that the dielectric medium would better be represented by a complex function rather than by a constant.⁵³ Table 6 shows the energies of the stationary points of Table 1 (except for mechanism II-6S) when the SMD values with $\epsilon = 4$ are added. One can observe that the presence of the dielectric medium slightly increases the energy values shown in Table 1 but that the ordering is kept in all cases. So, all the conclusions reached using the theozyme model are still valid.

The precedent results show that the mechanism of the peptide release process is still an unsolved problem and the possibility of a two-step reaction cannot be disregarded. In fact, a quite recent paper of Rodnina's group⁵⁴ strengthens the complexity of the puzzle through the study of proton inventories (reaction rates measured in buffers with increasing content of deuterated water). They find that the proton inventory for the RF2 dependent reaction shows a linear relationship, this fact being consistent with a model in which the reaction rate is limited for the formation of a single hydrogen bond. Thus, these results question the feasibility of the mechanisms suggested up to the present.

CONCLUSIONS

From the results obtained in this paper for the peptide release process we can conclude that the energy barriers for the two-step mechanisms are lower than the ones for the concerted process,¹² in such a way that the energy barriers of the determining step are now quite similar to the experimental ones. As in the case of the concerted mechanisms, the 2'OH plays an important catalytic role in the two steps. Another important point is the fact that the most favorable mechanisms we have found seem to confirm the ideas of the groups of Ramakrishnan^{18,21} and Aqvist,²⁵ which

propose that the side chain accommodates a nucleophilic water molecule in the PTC. In fact, the formation of the hydrogen bond not only accommodates the water molecule but also contributes to activate this molecule through electron transfer to the water oxygen. With regard to the second step, which is the rate-determining one, mechanisms II-6f1 and II-6w1 follow a quite different strategy to catalyze the reaction given that formamide forms a hydrogen bond with the O2 atom, while in mechanism II-6w1, the water molecule has migrated, leading to the formation of an eight-member cycle.

The main conclusion of our work is that the two-step mechanisms cannot be disregarded as usually are in the studies of the peptide release process, since they can contribute to clarify this complex and yet unsolved problem.

ASSOCIATED CONTENT

Supporting Information

Complete refs 37, 42, and 43, Cartesian coordinates of transition state structures, and absolute energies (in Hartree) for all the optimized structures. This material is available free of charge via the Internet at <http://pubs.acs.org>.

AUTHOR INFORMATION

Corresponding Author

*E-mail: bertran@klingon.uab.cat.

Notes

The authors declare no competing financial interest.

ACKNOWLEDGMENTS

Financial support from Ministerio de Economía y Competitividad (through Grants CTQ2011-24847 and CTQ2010-15408) and Generalitat de Catalunya (through Grants SGR2009-733 and XRQTC) and allowance of computer resources from the CESCA supercomputing center are gratefully acknowledged.

REFERENCES

- (1) Leung, E. K. Y.; Suslov, N.; Tuttle, N.; Sengupta, R.; Piccirilli, J. A. The Mechanism of Peptidyl Transfer Catalysis by the Ribosome. *Annu. Rev. Biochem.* **2011**, *80*, 527–555.
- (2) Youngman, E. M.; McDonald, M. E.; Green, R. Peptide Release on the Ribosome: Mechanism and Implications for Translational Control. *Annu. Rev. Microbiol.* **2008**, *62*, 353–373.
- (3) Zavialov, A. V.; Mora, L.; Buckingham, R. H.; Ehrenberg, M. Release of Peptide Promoted by the GGQ Motif of Class 1 Release Factors Regulates the GTPase Activity of RF3. *Molecular Cell* **2002**, *10*, 789–798.
- (4) Rawat, U. B. S.; Zavialov, A. V.; Sengupta, J.; Valle, M.; Grassucci, R. A.; Linde, J.; Vestergaard, B.; Ehrenberg, M.; Frank, J. A Cryo-Electron Microscopic Study of Ribosome-Bound Termination Factor RF2. *Nature* **2003**, *421*, 87–90.
- (5) Klaholz, B. P.; Pape, T.; Zavialov, A. V.; Myasnikov, A. G.; Orlova, E. V.; Vestergaard, B.; Ehrenberg, M.; Heel, M. v. Structure of the

Table 6. Relative Energies Obtained by Adding Solvation Free Energy ($\epsilon = 4$) to the Energies of the Stationary Points Corresponding to Two-Step Mechanisms

mechanism	energy	R	RC	TS1	Int1	Int2	TS2	PC	P
II-4	$\Delta E'$	0.0	-3.3	40.2	0.8	2.0	41.8	-2.7	4.0
II-6	$\Delta E'$	0.0	-6.5	27.7	-1.6	-1.6	32.7	-4.6	5.3
II-6w1	$\Delta E'$	0.0	-12.0	19.6	-7.7	-7.1	25.2	-7.4	2.5
II-6w2	$\Delta E'$	0.0	-7.5	25.5	-2.1	-2.1	30.5	-5.2	1.4
II-6f1	$\Delta E'$	0.0	-11.3	17.9	-7.5	-7.5	26.9	-10.9	0.6

Escherichia Coli Ribosomal Termination Complex with Release Factor 2. *Nature* **2003**, *421*, 90–94.

(6) Mora, L.; Heurgué-Hamard, V.; Champ, S.; Ehrenberg, M.; Kisselev, L. L.; Buckingham, R. H. The Essential Role of the Invariant GGQ Motif in the Function and Stability *in Vivo* of Bacterial Release Factors RF1 and RF2. *Mol. Microbiol.* **2003**, *47*, 267–275.

(7) Ma, B.; Nussinov, R. Release Factors eRF1 and RF2. A Universal Mechanism Controls the Large Conformational Changes. *J. Biol. Chem.* **2004**, *279*, 53875–53885.

(8) Shin, D. H.; Brandsen, J.; Jancarik, J.; Yokota, H.; Kim, R.; Kim, S.-H. Structural Analyses of Peptide Release Factor 1 from *Thermotoga Maritima* Reveal Domain Flexibility Required for its Interaction with the Ribosome. *J. Mol. Biol.* **2004**, *341*, 227–239.

(9) Petry, S.; Brodersen, D. E.; Murphy, F. V., IV; Dunham, C. M.; Selmer, M.; Tarry, M. J.; Kelley, A. C.; Ramakrishnan, V. Crystal Structures of the Ribosome in Complex with Release Factors RF1 and RF2 Bound to a Cognate Stop Codon. *Cell* **2005**, *123*, 1255–1266.

(10) Rawat, U.; Gao, H.; Zavialov, A.; Gursky, R.; Ehrenberg, M.; Frank, J. Interactions of the Release Factor RF1 with the Ribosome as Revealed by Cryo-EM. *J. Mol. Biol.* **2006**, *357*, 1144–1153.

(11) Ivanova, E. V.; Kolosov, P. M.; Birdsall, B.; Kelly, G.; Pastore, A.; Kisselev, L. L.; Polshakov, V. I. Eukaryotic Class 1 Translation Termination Factor eRF1. The NMR Structure and Dynamics of the Middle Domain Involved in Triggering Ribosome-Dependent Peptidyl-tRNA Hydrolysis. *FEBS J.* **2007**, *274*, 4223–4237.

(12) Acosta-Silva, C.; Bertran, J.; Branchadell, V.; Oliva, A. Quantum-Mechanical Study on the Mechanism of Peptide Release in the Ribosome. *J. Phys. Chem. B* **2013**, *117*, 3503–3515.

(13) Acosta-Silva, C.; Bertran, J.; Branchadell, V.; Oliva, A. Quantum-Mechanical Study on the Mechanism of Peptide Bond Formation in the Ribosome. *J. Am. Chem. Soc.* **2012**, *134*, 5817–5831.

(14) Zaher, H. S.; Shaw, J. J.; Strobel, S. A.; Green, R. The 2'-OH Group of the Peptidyl-tRNA Stabilizes an Active Conformation of the Ribosomal PTC. *EMBO J.* **2011**, *30*, 2445–2453.

(15) Weinger, J. S.; Parnell, K. M.; Dorner, S.; Green, R.; Strobel, S. A. Substrate-Assisted Catalysis of Peptide Bond Formation by the Ribosome. *Nat. Struct. Mol. Biol.* **2004**, *11*, 1101–1106.

(16) Brunelle, J. L.; Shaw, J. J.; Youngman, E. M.; Green, R. Peptide Release on the Ribosome Depends Critically on the 2'-OH of the Peptidyl-tRNA Substrate. *RNA* **2008**, *14*, 1526–1531.

(17) Schmeing, T. M.; Huang, K. S.; Kitchen, D. E.; Strobel, S. A.; Steitz, T. A. Structural Insights into the Roles of Water and the 2' Hydroxyl of the P Site tRNA in the Peptidyl Transferase Reaction. *Mol. Cell* **2005**, *20*, 437–448.

(18) Weixlbaumer, A.; Jin, H.; Neubauer, C.; Voorhees, R. M.; Petry, S.; Kelley, A. C.; Ramakrishnan, V. Insights into Translational Termination from the Structure of RF2 bound to the Ribosome. *Science* **2008**, *322*, 953–956.

(19) Laurberg, M.; Asahara, H.; Korostelev, A.; Zhu, J.; Trakhanov, S.; Noller, H. Structural Basis for Translation Termination on the 70S Ribosome. *Nature* **2008**, *454*, 852–857.

(20) Korostelev, A.; Asahara, H.; Lancaster, L.; Laurberg, M.; Hirschi, A.; Zhu, J.; Trakhanov, S.; Scott, W. G.; Noller, H. F. Crystal Structure of a Translation Termination Complex Formed with Release Factor RF2. *Proc. Natl. Acad. Sci. U.S.A.* **2008**, *105*, 19684–19689.

(21) Jin, H.; Kelley, A. C.; Loakes, D.; Ramakrishnan, V. Structure of the 70S Ribosome Bound to Release Factor 2 and a Substrate Analog Provides Insights into Catalysis of Peptide Release. *Proc. Natl. Acad. Sci. U.S.A.* **2010**, *107*, 8593–8598.

(22) Trobro, S.; Aqvist, J. Mechanism of Peptide Bond Synthesis on the Ribosome. *Proc. Natl. Acad. Sci. U.S.A.* **2005**, *102*, 12395–12400.

(23) Trobro, S.; Aqvist, J. Analysis of Predictions for the Catalytic Mechanism of Ribosomal Peptidyl Transfer. *Biochemistry* **2006**, *45*, 7049–7056.

(24) Trobro, S.; Aqvist, J. A Model for how Ribosomal Release Factors Induce Peptidyl-tRNA Cleavage in Termination of Protein Synthesis. *Mol. Cell* **2007**, *27*, 758–766.

(25) Trobro, S.; Aqvist, J. Mechanism of the Translation Termination Reaction on the Ribosome. *Biochemistry* **2009**, *48*, 11296–11303.

(26) Song, H.; Mugnier, P.; Das, A. K.; Webb, H. M.; Evans, D. R.; Tuite, M. F.; Hemmings, B. A.; Barford, D. The Crystal Structure of Human Eukaryotic Release Factor eRF1. Mechanism of Stop Codon Recognition and Peptidyl-tRNA Hydrolysis. *Cell* **2000**, *100*, 311–321.

(27) Korostelev, A.; Zhu, J.; Asahara, H.; Noller, H. F. Recognition of the Amber UAG Stop Codon by Release Factor RF1. *EMBO J.* **2010**, *29*, 2577–2585.

(28) Carrasco, N.; Hiller, D. A.; Strobel, S. A. Minimal Transition State Charge Stabilization of the Oxyanion during Peptide Bond Formation by the Ribosome. *Biochemistry* **2011**, *50*, 10491–10498.

(29) Shaw, J. J.; Green, R. Two Distinct Components of Release Factor Function Uncovered by Nucleophile Partitioning Analysis. *Mol. Cell* **2007**, *28*, 458–467.

(30) Rangelov, M. A.; Vayssilov, G. N.; Yomtova, V. M.; Petkov, D. D. The syn-Oriented 2-OH Provides a Favorable Proton Transfer Geometry in 1,2-Diol Monoester Aminolysis: Implications for the Ribosome Mechanism. *J. Am. Chem. Soc.* **2006**, *128*, 4964–4965.

(31) Wang, Q.; Gao, J.; Liu, Y.; Liu, C. Validating a new Proton Shuttle Reaction Pathway for Formation of the Peptide Bond in Ribosomes: A Theoretical Investigation. *Chem. Phys. Lett.* **2010**, *501*, 113–117.

(32) Byun, B. J.; Kang, Y. K. A Mechanistic Study Supports a Two-Step Mechanism for Peptide Bond Formation on the Ribosome. *Phys. Chem. Chem. Phys.* **2013**, *15*, 14931–14935.

(33) Zhao, Y.; Truhlar, D. G. The M06 Suite of Density Functionals for Main Group Thermochemistry, Thermochemical Kinetics, Non Covalent Interactions, Excited States and Transition Elements: Two New Functionals and Systematic Testing of Four M06-Class Functionals and 12 other Functionals. *Theor. Chem. Acc.* **2008**, *120*, 215–241.

(34) Zhao, Y.; Truhlar, D. G. Density Functionals with Broad Applicability in Chemistry. *Acc. Chem. Res.* **2008**, *41*, 157–167.

(35) Marenich, A. V.; Cramer, C. J.; Truhlar, D. G. Universal Solvation Model Based on Solute Electron Density and on a Continuum Model of the Solvent Defined by the Bulk Dielectric Constant and Atomic Surface Tensions. *J. Phys. Chem. B* **2009**, *113*, 6378–6396.

(36) McQuarrie, D. A. *Statistical Mechanics*; Harper & Row: New York, 1986.

(37) Frisch, M. J.; Trucks, G. W.; Schlegel, H. B.; Scuseria, G. E.; Robb, M. A.; Cheeseman, J. R.; Scalmani, G.; Barone, V.; Mennucci, B.; Petersson, G. A. et al. *Gaussian 09*, revision B.01; Gaussian, Inc.: Wallingford, CT, 2009.

(38) Reed, A. E.; Curtiss, L. A.; Weinhold, F. Intermolecular Interactions from a Natural Bond Orbital, Donor-Acceptor Viewpoint. *Chem. Rev.* **1988**, *88*, 899–926.

(39) Tantillo, D. J.; Chen, J.; Houk, K. N. Theozymes and Compuzymes: Theoretical Models for Biological Catalysis. *Curr. Opin. Chem. Biol.* **1998**, *2*, 743–750.

(40) DeChancie, J.; Clemente, F. R.; Smith, A. J. T.; Gunaydin, H.; Zhao, Y.-L.; Zhang, X.; Houk, K. N. How Similar are Enzyme Active Site Geometries Derived from Quantum Mechanical Theozymes to Crystal Structures of Enzyme-Inhibitor Complexes? Implications for Enzyme Design. *Protein Sci.* **2007**, *16*, 1851–1866.

(41) Zhang, X.; DeChancie, J.; Gunaydin, H.; Chowdry, A. B.; Clemente, F. R.; Smith, A. J. T.; Handel, T. M.; Houk, K. N. Quantum Mechanical Design of Enzyme Active Sites. *J. Org. Chem.* **2008**, *73*, 889–899.

(42) Rothlisberger, D.; Khersonsky, O.; Wollacott, A. M.; Jiang, L.; DeChancie, J.; Betker, J.; Gallaher, J. L.; Althoff, E. A.; Zanghellini, A.; Dym, O.; et al. Kemp Elimination Catalysts by Computational Enzyme Design. *Nature* **2008**, *453*, 190–195.

(43) Jiang, L.; Althoff, E. A.; Clemente, F. R.; Doyle, L.; Rothlisberger, D.; Zanghellini, A.; Gallaher, J. L.; Betker, J.; Tanaka, F.; Barbas, C. F., III; et al. De Novo Computational Design of Retro-Aldol Enzymes. *Science* **2008**, *319*, 1387–1391.

(44) Hilvert, D. Design of Protein Catalysts. *Annu. Rev. Biochem.* **2013**, *82*, 447–470.

(45) Hratchian, H. P.; Schlegel, H. B. Accurate Reaction Paths Using a Hessian Based Predictor-Corrector Integrator. *J. Chem. Phys.* **2004**, *120*, 9918–9925.

- (46) Page, M. I.; Jencks, W. P. Entropic Contributions to Rate Accelerations in Enzymic Intramolecular Reactions and the Chelate Effect. *Proc. Natl. Acad. Sci. U.S.A.* **1971**, *68*, 1678–1683.
- (47) Kim, Y.; Mohrig, J. R.; Truhlar, D. G. Free-Energy Surfaces for Liquid-Phase Reactions and their Use to Study the Border Between Concerted and Nonconcerted α,β -Elimination Reactions of Esters and Thioesters. *J. Am. Chem. Soc.* **2010**, *132*, 11071–11082.
- (48) Wiberg, K. B. Application of the Pople-Santry-Segal CNDO Method to the Cyclopropylcarbanyl and Cyclobutyl Cation and to Bicyclobutane. *Tetrahedron* **1968**, *24*, 1083–1096.
- (49) Youngman, E. L.; Brunelle, J. L.; Kochaniak, A. B.; Green, R. The Active Site of the Ribosome is Composed of Two Layers of Conserved Nucleotides with Distinct Roles in Peptide Bond Formation and Peptide Release. *Cell* **2004**, *117*, 589–599.
- (50) Smith, A. J. T.; Müller, R.; Toscano, M. D.; Kast, P.; Hellinga, H. W.; Hilvert, D.; Houk, K. N. Structural Reorganization and Preorganization in Enzyme Active Sites: Comparisons of Experimental and Theoretically Ideal Active Site Geometries in the Multistep Serine Esterase Reaction Cycle. *J. Am. Chem. Soc.* **2008**, *130*, 15361–15373.
- (51) Hammes, G. G.; Benkovic, S. J.; Hammes-Schiffer, S. Flexibility, Diversity, and Cooperativity: Pillars of Enzyme Catalysis. *Biochemistry* **2011**, *50*, 10422–10430.
- (52) Siegbahn, E. M.; Blomberg, M. R. A. Transition-Metal Systems in Biochemistry Studies by High-Accuracy Quantum Chemical Methods. *Chem. Rev.* **2000**, *100*, 421–437.
- (53) Li, L.; Li, C.; Zhang, Z.; Alexov, E. On the Dielectric “Constant” of Proteins: Smooth Dielectric Function for Macromolecular Modeling and Its Implementation in DelPhi. *J. Chem. Theory Comput.* **2013**, *9*, 2126–2136.
- (54) Kuhlencoetter, S.; Wintermeyer, W.; Rodnina, M. V. Different Substrate-Dependent Transition States in the Active Site of the Ribosome. *Nature* **2011**, *476*, 351–354.